A coarse-grain model for cellular growth accounting for ribosome synthesis

Massimiliano d'Angelo[1,2], Pasquale Palumbo[1,3,4,†], Stefano Busti[1,3] and Marco Vanoni[1,3]

***Abstract*— Protein synthesis in eukaryotes is carried out by ribosomes, large RNA–protein complexes consisting of a small and a large subunit. In this work we present a mathematical model for cellular growth comprising both protein production and ribosome synthesis, properly accounting for both small and large subunits dynamics. The qualitative analysis of the model is carried out according to a simplifying assumption on the proportion of the two ribosomal subunits in stationary growth conditions; such hypothesis is based on a reasonable biological ground. Conditions are given on the model parameters in order to ensure exponential growth and the corresponding growth rate is straightforwardly computed from the model parameters. These results are validated by numerical simulations carried out according to a set of biologically meaningful model parameters. The modified model is better suited to host molecular blow-up of ribosomal synthesis and cell growth within a modular whole-cell model able to act as a scaffold connecting metabolism, growth and cycle.**

I. INTRODUCTION

RNA and proteins account for over 70% of cell biomass (`http://book.bionumbers.org/what-is-the-macromolecular-composition-of-the-cell/`). In living cells protein synthesis is carried out by ribosomes, large RNA-protein macromolecular complexes consisting of a Small SubUnit (SSU) and a Large SubUnit (LSU). The scheme reported in Fig.1 shows that one SSU and one LSU interact with one messenger RNA (mRNA) molecule yielding a mature ribosome ready for protein translation. Amino acids are carried by transfer RNA (tRNA). The process repeats several times leading to the synthesis of a protein. Once synthesis of the protein is terminated, the complex dissociates into free ribosomal subunits, the synthesized protein and the mRNA. Many of the biochemical details related to ribosome synthesis and protein production have been elucidated over the last decades (see *e.g.* [1]), showing that, at a molecular level, synthesis, degradation and regulation are emergent properties arising from complex interconnected networks.

The ribosome/protein syntesis model - originally described in [2] - belongs to an integrated low-granularity model [3] interconnecting yeast Metabolism, Growth and Cell Cycle. It can be used as a scaffold for molecularly detailed models of the yeast functions, such as a molecular model of ribosome biosynthesis. Each ribosome is made of two subunits (Figure 1) and the assembly of each subunit is a complex process requiring several hundreds of gene products. The integrated model belongs to the category of whole-cell-models, pioneered by [4].

The elaborate process of ribosome bio-genesis (ribosome assembly) has been thoroughly investigated at the molecular level (mostly in bacteria and yeast cells) and a large number of molecular players involved in the assembly of both subunits have been identified (*e.g.* [5], [6]). The first step in the molecular reconstruction of this process is a low-granularity model that implements separately biosynthesis of the two subunits. Accordingly, this note proposes a low granularity Ordinary Differential Equation (ODE) model of ribosome/protein production as an extension of [2] that accounts for small and large ribosomal subunits dynamics.

Similarly to [7] where an accurate qualitative behavior analysis has been carried out on the model in [2]), here we investigate the conditions on the parameters of the new model that ensure exponential growth. Differently from [2], [7], here we have nonlinearities that prevent straightforward computations. Therefore, the qualitative behavior analysis is carried out according to the simplifying assumption that small and large subunits are in equi-molar proportion in exponential growth conditions. This fact is supported on a solid biological ground [9,10] and allows to reduce the complexity of the model. Conditions are given on the reduced-order model parameters that ensure stationary exponential growth and the corresponding growth rate is straightforwardly computed from the model parameters. These results are validated by numerical simulations carried out according to a set of biologically meaningful model parameters.

II. RIBOSOME-PROTEIN SYNTHESIS MODEL

The proposed model builds upon the following coarse-grain ribosome-protein synthesis model presented in [2] (and exploited more recently in [3] as a growth module in the skeleton of a yeast whole-cell model integrating metabolism, growth and cycle). In the next subsection, we briefly recall its mathematical structure.

A. The low-granularity growth model [2]

Let R_{tot} and P be the copy numbers of ribosomes[1] and proteins (these last in terms of polymerized amino acids).

[1]Department of Biotechnology and Biosciences, University of Milano-Bicocca, 20126 Milan, Italy.

[2]current affiliation: Department of Computer, Control, and Management Engineering "Antonio Ruberti", Sapienza University of Rome, 00185 Rome, Italy

[3]SYSBIO- ISBE, 20126 Milan, Italy.

[4]Istituto di Analisi dei Sistemi e Informatica "A. Ruberti", Italian National Research Council (IASI-CNR), Rome, Italy.

†Corresponding author, `pasquale.palumbo@unimib.it`

[1]We use the subscript *tot*, standing for *total number*, for what we introduce later.

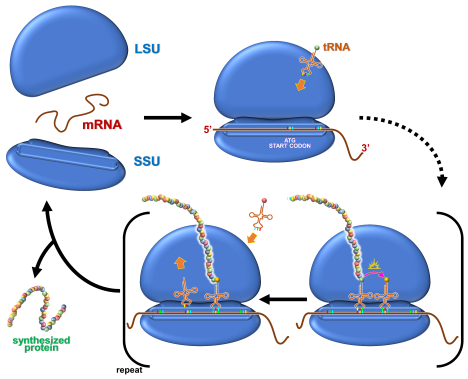

Fig. 1. Schematic representation of the ribosome cycle.

The growth model proposed in [2] is described by the following equations

$$\dot{R}_{\text{tot}} = K_1(\rho P - R_{\text{tot}})^+ - \frac{1}{T_1}R_{\text{tot}}, \tag{1}$$

$$\dot{P} = K_2 R - \frac{1}{T_2}P, \tag{2}$$

where the nonlinear function $(\cdot)^+$ is the positive part, *i.e.* $(x)^+ = x$ if $x \geq 0$ and $(x)^+ = 0$ if $x < 0$, and K_1, T_1, K_2, T_2 are positive model parameters, whose values may vary according to environmental conditions (*e.g.* nutrients). In particular, K_1 and K_2 are the average total ribosome assembly efficiency and the translational efficiency respectively, while T_1 and T_2 are the ribosomes and proteins degradation time constants, respectively.

Both dynamics come out from the balance between synthesis and degradation. With regard to the ribosome synthesis, a negative feedback is assumed to control the synthesis rate according to the ribosomes-over-proteins ratio [8], [2], [9]: if the ratio R_{tot}/P overcomes a threshold ρ (*i.e.*, if there are too many ribosomes with respect to the actual quantity of proteins) there is no ribosome synthesis; otherwise, the ribosome synthesis is proportional to the (positive) difference $\rho P(t) - R_{\text{tot}}(t)$. With regard to the protein production rate, it is assumed a linear transformation of the ribosome content. Both ribosomes and proteins degradation rates are linear.

We refer the interested reader to [7] for an extensive qualitative analysis of the model (1)–(2).

B. Small and large ribosomal subunits

Ribosomes are large RNA–protein macromolecular complexes consisting of a Small and a Large Sub-Unit (SSU and LSU, respectively). During protein synthesis, the small subunit binds to the large subunit onto the mRNA strand with peptide-bond formation (see Fig. 1).

Our proposed model characterizes the dynamics of the following cellular components:

R_{SSU} : copy number of free SSU
R_{LSU} : copy number of free LSU
R : copy number of active ribosomes
P : copy number of polymerized amino acids

By *free* SSU/LSU we refer to the components that are not bound together onto the mRNA strand. Contrarily, by *active* ribosomes we refer to the macromolecule provided by one SSU and one LSU bound together onto the mRNA strand in the process of translation, according to the following binding/unbinding reaction

$$R_{\text{SSU}} + R_{\text{LSU}} \underset{k_{\text{off}}}{\overset{\tilde{k}_{\text{on}}}{\rightleftharpoons}} R, \tag{3}$$

where $\tilde{k}_{\text{on}}$ and k_{off} are the binding/unbinding reaction rate constants. Thus, the total number of ribosomes is defined as

$$R_{\text{tot}} = R + \min\{R_{\text{SSU}}, R_{\text{LSU}}\}. \tag{4}$$

Remark. Although, from a biological viewpoint, the binding/unbinding reaction (3) requires the presence of an mRNA strand, the proposed model neglects it, assuming that there is plenty of mRNA slots where ribosomal subunits may bind. Indeed, dealing, *e.g.*, with a yeast cell accounting for an average number of $3.6 \cdot 10^4$ mRNA strands, we have that about 71% is busy with ribosomes (in average 5 ribosomes per mRNA strand out of an overall number of 8 contemporary binding sites per mRNA strand), so that there can be found an average number of free-from-ribosomes mRNA slots equal to

$$0.71 \times 3.6 \cdot 10^4 \times (8-5) + 0.29 \times 3.6 \cdot 10^4 \times 8 = 1.6 \cdot 10^5$$

Such number is one order of magnitude greater than the unbound ribosomes (*i.e.* pairs of unbound small/large subunits) equal to $3.75 \cdot 10^4$ (about 15% of the overall number of ribosomes) [10], [11], [12], [13], [14], [15].

C. The ribosomes/proteins synthesis model

In the following, we exploit the usual *square brackets* notation to indicate concentrations. By denoting with V the volume of a growing cell, from (3) the ribosomes dynamics may be written, according to *mass action law* [16], with respect to concentrations, as

$$[\dot{R}] = \tilde{k}_{\text{on}}[R_{\text{SSU}}][R_{\text{LSU}}] - k_{\text{off}}[R] - \frac{[R]}{V}\dot{V}, \tag{5}$$

where the last term of the right-hand-side of (5) is the dilution term and it takes into account the cell volume variation. Keeping in mind the relationship between amounts and concentrations (*e.g.* $R = V[R]$ for ribosomes), the ODE (5) may be re-written in terms of copy numbers

$$\begin{aligned}\dot{R} &= \dot{V}[R] + V[\dot{R}] \\ &= \dot{V}[R] + \tilde{k}_{\text{on}}V[R_{\text{SSU}}][R_{\text{LSU}}] - k_{\text{off}}V[R] - [R]\dot{V} \\ &= \tilde{k}_{\text{on}}\frac{R_{\text{SSU}}R_{\text{LSU}}}{V} - k_{\text{off}}R.\end{aligned} \tag{6}$$

Moreover, we assume that the cell volume is proportional to the number of the proteins, [17], through the factor α, namely $V = \alpha P$, thus we obtain

$$\dot{R} = k_{\text{on}}\frac{R_{\text{SSU}}R_{\text{LSU}}}{P} - k_{\text{off}}R, \tag{7}$$

with $k_{\text{on}} = \tilde{k}_{\text{on}}/\alpha$.

Similarly to the ribosome synthesis modeled by (1) in [2], both small and large subunits synthesis is switched off in case the overall ribosomes-over-protein ratio exceeds a given threshold ρ. Thus, from the binding/unbinding reaction (3), we describe the dynamics of the two subunits as follows

$$\dot{R}_{\text{SSU}} = k_{\text{SSU}} \left(\rho P - R_{\text{tot}}\right)^+ - \gamma_{\text{SSU}} R_{\text{SSU}} - k_{\text{on}} \frac{R_{\text{SSU}} R_{\text{LSU}}}{P} + k_{\text{off}} R, \quad (8)$$

$$\dot{R}_{\text{LSU}} = k_{\text{LSU}} \left(\rho P - R_{\text{tot}}\right)^+ - \gamma_{\text{LSU}} R_{\text{LSU}} - k_{\text{on}} \frac{R_{\text{SSU}} R_{\text{LSU}}}{P} + k_{\text{off}} R, \quad (9)$$

where k_{SSU}, k_{LSU}, γ_{SSU}, γ_{LSU} are positive parameters, whose values may vary according to environmental conditions (*e.g.* nutrients).

Notice that there is no explicit degradation for active ribosomes, whose clearance passes through the unbinding of the two sub-units [16].

Finally, we model the proteins synthesis as in (2):

$$\dot{P} = K_2 R - \gamma_p P \quad (10)$$

with γ_p playing the same role of $1/T_2$ in (2).

To summarize, equations (7), (8), (9) and (10) constitute the ODEs of the new ribosome-protein synthesis model.

III. GROWTH RATE COMPUTATION

In the previous section we discussed the rationale behind the new ribosome-protein synthesis model. Here we investigate according to which parameter conditions we obtain exponential growth, and how to compute the growth rate from the model parameter values.

A. Reduced order model

Due to the nonlinearities of the model equations, we introduce the simplifying assumption that, in exponential growth conditions, the number of ribosomal SSU and LSU is approximately the same, namely

$$R_{\text{SSU}} \approx R_{\text{LSU}}. \quad (11)$$

Indeed, Since ribosome biogenesis is energetically costly, several mechanisms ensure that the synthesis of the two subunit and their components are well balanced to prevent impairment of growth and cell cycle arrest (nucleolar-stress response [8]). Block of the Large SubUnit (LSU) assembly interrupts accumulation of the Small SubUnit (SSU) assembly, whereas halting the SSU synthesis leads to the accumulation of a partly degraded LSU [18]. Finally, the turnover ratio of the ribosomal proteins of both subunits is similar (10 h) [19].

As a consequence, by (8) and (9) it is possible to reduce the state space of the model into three state variables only. To this end we assume

$$k_{\text{SSU}} \simeq k_{\text{LSU}}, \qquad \gamma_{\text{SSU}} \simeq \gamma_{\text{LSU}} \quad (12)$$

and replace the two subunits dynamics with a unique one, R_{SU} namely, accounting for both:

$$\dot{R}_{\text{SU}} = k_{\text{SU}} \left(\rho P - R_{\text{tot}}\right)^+ - \gamma_{\text{SU}} R_{\text{SU}} - k_{\text{on}} \frac{R_{\text{SU}}^2}{P} + k_{\text{off}} R, \quad (13)$$

with parameters $k_{\text{SU}} = k_{\text{SSU}} \simeq k_{\text{LSU}}$ and $\gamma_{\text{SU}} = \gamma_{\text{SSU}} \simeq \gamma_{\text{LSU}}$. Consequently, the number of total ribosomes is given by

$$R_{\text{tot}} = R + R_{\text{SU}}. \quad (14)$$

In summary, the reduced order model is now provided by (13) together with the updated (7) and (10):

$$\begin{aligned} \dot{R}_{\text{SU}} &= k_{\text{SU}} \left(\rho P - R - R_{\text{SU}}\right)^+ - \gamma_{\text{SU}} R_{\text{SU}} - k_{\text{on}} \frac{R_{\text{SU}}^2}{P} + k_{\text{off}} R \\ \dot{R} &= k_{\text{on}} \frac{R_{\text{SU}}^2}{P} - k_{\text{off}} R, \\ \dot{P} &= K_2 R - \gamma_p P. \end{aligned} \quad (15)$$

Finally, we notice that from (15) the degradation of R_{tot} is proportional just to R_{SU} and not to R_{tot}, which is able to catch the biological fact that the degradation of the total number of ribosomes is proportional to the "inactive" subunits only, whilst the "active" ribosomes are synthesizing for proteins and cannot be degraded.

B. Exponential growth conditions

In exponential growth conditions, all cellular players grow according to the same exponential growth, so that, if (15) admits exponential growth conditions, at *regime* the ratios

$$\frac{R_{\text{SU}}}{P}, \qquad \frac{R}{P}, \qquad \frac{R_{\text{SU}}}{R} \quad (16)$$

converge to stationary values. The following Theorem is the main result of the manuscript and proves that, provided a set of sufficient conditions hold true, we actually obtain exponential growth for system (15).

Theorem 1: Assume that the model parameters in (15) satisfy the following constraints

$$\sqrt{\frac{k_{\text{off}} \gamma_p}{k_{\text{on}} K_2}} < \rho - \frac{\gamma_p}{K_2} \quad (17)$$

$$k_{\text{SU}} > k_{\text{off}} \quad (18)$$

$$(k_{\text{SU}} + \gamma_{\text{SU}}) \sqrt{\frac{k_{\text{off}} \gamma_p}{k_{\text{on}} K_2}} + \frac{k_{\text{SU}} \gamma_p}{K_2} \leq \rho k_{\text{SU}} \quad (19)$$

$$\rho(K_2 \rho - \gamma_p) - (K_2 \rho - \gamma_{\text{SU}}) \tilde{\beta} \geq 0 \quad (20)$$

with $\tilde{\beta}$ provided by

$$\tilde{\beta} = \frac{-(2K_2 \rho + k_{\text{off}} - \gamma_p) + \sqrt{\Delta}}{2(k_{\text{on}} - K_2)} \qquad \text{and} \quad (21)$$

$$\Delta = (k_{\text{off}} - \gamma_p)^2 + 4\rho k_{\text{on}} (k_{\text{off}} - \gamma_p + \rho K_2) \geq 0 \quad (22)$$

Then, there exists exponential growth for (15) with, at *regime*

$$\frac{R_{\text{SU}}}{P} = \beta \quad (23)$$

where β is the unique solution of

$$\psi(\beta) = \rho \, k_{\text{SU}} \qquad \text{with} \quad (24)$$

$$\psi(\beta) = k_{\text{on}}\beta^2 + \big(\lambda_+(\beta) + k_{\text{SU}} + \gamma_{\text{SU}}\big)\beta + \frac{(k_{\text{SU}} - k_{\text{off}})\big(\lambda_+(\beta) + \gamma_p\big)}{K_2} \qquad \text{and} \tag{25}$$

$$\lambda_+(\beta) = \frac{-(k_{\text{off}} + \gamma_p) + \sqrt{(k_{\text{off}} - \gamma_p)^2 + 4\beta^2 k_{\text{on}} K_2}}{2}. \tag{26}$$

is the exponential growth rate shared by R_{SU}, R and P at *regime*.

Proof: The proof starts by showing that the constraint (23) is compatible with the solution at *regime*. To this end, by substituting (23) in the ribosome dynamics (15):

$$\dot{R} = k_{\text{on}}\beta^2 P - k_{\text{off}} R \tag{27}$$

we have that the (R, P) dynamics may be described by the following second-order, linear system:

$$\dot{x} = Ax, \tag{28}$$

where,

$$x = \begin{bmatrix} R \\ P \end{bmatrix}, \quad A = \begin{bmatrix} -k_{\text{off}} & \beta^2 k_{\text{on}} \\ K_2 & -\gamma_p \end{bmatrix}. \tag{29}$$

with the characteristic polynomial $p(\lambda)$ associated to A:

$$p(\lambda) = \det(\lambda I - A) = \lambda^2 + (\gamma_p + k_{\text{off}})\lambda + k_{\text{off}}\gamma_p - \beta^2 k_{\text{on}} K_2.$$

From the Hurwitz stability criterion it is easy to see that the existence of a unique positive real root is ensured by the constraint

$$k_{\text{off}}\gamma_p - \beta^2 k_{\text{on}} K_2 < 0, \tag{30}$$

that is

$$\beta > \sqrt{\frac{k_{\text{off}}\,\gamma_p}{k_{\text{on}}\,K_2}} =: \beta_* \tag{31}$$

with the positive real eigenvalue, denoted by λ_+ given by (26). Instead, if (31) is not true, then both eigenvalues are negative real, and there is no exponential growth. The point is to check whether such a β exists, and how to compute it. Assuming such existence, according to the spectral decomposition of matrix A, by denoting with u and $v^\top$ the right and left eigenvectors of A associated to λ_+, respectively, the evolutions of R and P are given, at *regime* by

$$\begin{bmatrix} R \\ P \end{bmatrix} = \mathrm{e}^{\lambda_+ t} u\, v^\top \begin{bmatrix} R_0 \\ P_0 \end{bmatrix}, \tag{32}$$

where R_0, P_0 are the ribosomes and proteins initial conditions. Thus, accounting for the following positions

$$u = \begin{bmatrix} u_R \\ u_P \end{bmatrix}, \quad v^\top = [v_R \;\; v_P], \qquad \chi_0 = v^\top \begin{bmatrix} R_0 \\ P_0 \end{bmatrix} \tag{33}$$

it is $R(t) = \mathrm{e}^{\lambda_+ t} u_R \chi_0$ and $P(t) = \mathrm{e}^{\lambda_+ t} u_P \chi_0$. Moreover, by properly exploiting the eigenvalue/eigenvector identities $(\lambda_+ I - A)u = 0$, $v^\top(\lambda_+ I - A) = 0^\top$, one obtains

$$u_R = \frac{\lambda_+ + \gamma_p}{K_2} u_P, \qquad v_P = \frac{\lambda_+ + k_{\text{off}}}{K_2} v_R \tag{34}$$

It is worth noting that, according to *regime* solutions (32), it follows that the ratio R/P asymptotically converges to a stationary value.

By further substituting (23) into the R_{SU} dynamics in (15):

$$\beta\dot{P} = k_{\text{SU}}\big((\rho - \beta)P - R\big)^+ - \beta(\gamma_{\text{SU}} + k_{\text{on}}\beta)P + k_{\text{off}} R$$

By considering the *regime* equations (32), then after simplifications we have

$$\beta\lambda_+ u_P = k_{\text{SU}}\big((\rho - \beta)u_P - u_R\big)^+ - \beta(\gamma_{\text{SU}} + k_{\text{on}}\beta)u_P + k_{\text{off}} u_R,$$

where χ_0 has been put aside of the positive part function $(\cdot)^+$ and, then, simplified because, according to (33) and (34), the components of the eigenvectors associated to λ_+ may be chosen positive element-wise. Furthermore, accounting for (34) we have

$$\beta\lambda_+ = k_{\text{SU}}\left(\rho - \beta - \frac{\lambda_+ + \gamma_p}{K_2}\right)^+ - \beta(\gamma_{\text{SU}} + k_{\text{on}}\beta) + k_{\text{off}}\frac{\lambda_+ + \gamma_p}{K_2}. \tag{35}$$

In summary, solutions of the type (23) are compatible with the second-order linear system (28)-(29) for ribosomes/proteins dynamics, with β provided by the solution of the algebraic equation (35). Therefore, we need to characterize the solutions of (35) with respect to β, and to find out whether there exist solutions such that inequality (31) is guaranteed (*i.e.* ensuring a exponential growth).

In order to deal with the positive part function in (35), condition (17) allows to show that there exist $\tilde{\beta} \geq \beta_*$ such that for $\beta \in [\beta_*, \tilde{\beta}]$ it is

$$\rho - \beta - \frac{\lambda_+(\beta) + \gamma_p}{K_2} \geq 0 \tag{36}$$

Indeed, by explicitly accounting for the eigenvalue expression reported in (26), inequality (36) writes as

$$\varphi(\beta) \leq \rho + \frac{k_{\text{off}} - \gamma_p}{2K_2} \tag{37}$$

with

$$\varphi(\beta) = \beta + \frac{\sqrt{(k_{\text{off}} - \gamma_p)^2 + 4\beta^2 k_{\text{on}} K_2}}{2K_2} \tag{38}$$

a monotonically increasing function with respect to β, such that

$$\varphi(\beta_*) = \sqrt{\frac{k_{\text{off}}\gamma_p}{k_{\text{on}}K_2}} + \frac{k_{\text{off}} + \gamma_p}{2K_2}. \tag{39}$$

As a matter of fact, if (17) holds true, then

$$\varphi(\beta_*) \leq \rho + \frac{k_{\text{off}} - \gamma_p}{2K_2}. \tag{40}$$

Then, since $\lim_{\beta \mapsto +\infty} \varphi(\beta) = +\infty$, there exists a unique $\tilde{\beta} \geq \beta_*$ such that

$$\varphi(\tilde{\beta}) = \rho + \frac{k_{\text{off}} - \gamma_p}{2K_2} \tag{41}$$

and inequalities (37), and so (36), hold true for $\beta \in [\beta_*, \tilde{\beta}]$.

The explicit computation of $\tilde{\beta}$ follows from equations (38) and (41), namely

$$\sqrt{(k_{\text{off}} - \gamma_p)^2 + 4\tilde{\beta}^2 k_{\text{on}} K_2} = 2K_2(\rho - \tilde{\beta}) + k_{\text{off}} - \gamma_p. \tag{42}$$

By making the square and, after straightforward simplifications:

$$k_{\text{on}}\tilde{\beta}^2 = K_2(\rho-\tilde{\beta})^2 + (\rho-\tilde{\beta})(k_{\text{off}}-\gamma_p) \tag{43}$$

so that the following second-order equation is achieved for $\tilde{\beta}$:

$$(k_{\text{on}}-K_2)\tilde{\beta}^2+(2K_2\rho+k_{\text{off}}-\gamma_p)\tilde{\beta}-\rho(K_2\rho+k_{\text{off}}-\gamma_p)=0 \tag{44}$$

The existence of a unique real solution for $\tilde{\beta} \geq \beta_*$ allows to assume true the constraint for Δ in (22), according to which, $\tilde{\beta}$ in (21) follows from (44).

Then, according to (36), equation (35) becomes (24) with ψ given by (25). We finally have to prove that, provided conditions (18)-(20) hold true, then it is $\psi'(\beta) \geq 0$ in $[\beta_*, \tilde{\beta}]$ with

$$\psi(\beta_*) \leq \rho k_{\text{SU}} \leq \psi(\tilde{\beta}) \tag{45}$$

so that there exists a unique $\beta \in [\beta_*, \tilde{\beta}]$ satisfying (24). Since $\lambda_+(\beta_*)=0$, it is straightforward to note that

$$\psi(\beta_*) = k_{\text{on}}\beta_*^2 + (k_{\text{SU}}+\gamma_{\text{SU}})\beta_* + \frac{(k_{\text{SU}}-k_{\text{off}})\gamma_p}{K_2} \tag{46}$$

that is, according to (31):

$$\psi(\beta_*) = (k_{\text{SU}}+\gamma_{\text{SU}})\sqrt{\frac{k_{\text{off}}\gamma_p}{k_{\text{on}}K_2}} + \frac{k_{\text{SU}}\gamma_p}{K_2} \tag{47}$$

so that, because of hypothesis (19), it is $\psi(\beta_*) \leq \rho k_{\text{SU}}$. On the other hand, when $\beta = \tilde{\beta}$, (36) holds true as an equality, so that $\lambda_+(\tilde{\beta}) = K_2(\rho-\tilde{\beta})-\gamma_p$ and, after computations:

$$\begin{aligned}\psi(\tilde{\beta}) = (k_{\text{on}}-K_2)\tilde{\beta}^2 + (K_2\rho-\gamma_p+\gamma_{\text{SU}}+k_{\text{off}})\tilde{\beta} \\ +(k_{\text{SU}}-k_{\text{off}})\rho.\end{aligned} \tag{48}$$

By further exploiting (44), $\psi(\tilde{\beta})$ simplifies into:

$$\psi(\tilde{\beta}) = -(K_2\rho-\gamma_{\text{SU}})\tilde{\beta} + \rho(K_2\rho+k_{\text{SU}}-\gamma_p). \tag{49}$$

In summary, according to (49), from hypothesis (20), it is $\psi(\tilde{\beta}) \geq \rho k_{\text{SU}}$. Finally by computing the derivative $\psi'(\beta)$, it is easy to see from (18) and since $\lambda'_+(\beta)$ is greater than zero from (26), it follows that also $\psi'(\beta) \geq 0$ for any value of $\beta \in [\beta_*, \tilde{\beta}]$. ■

IV. NUMERICAL SIMULATIONS

Reported simulations have a twofold purpose. From the one hand, they aim at showing that the parameters of the proposed model (7)-(10) (*Refined Ribosome Synthesis model*, RRS for short) can be properly set in order to replicate the same features of the coarser model provided by (1)–(2) (*Coarse-grain Ribosome Synthesis model*, CRS for short): this is a mandatory starting point when building model extensions according to an increasing granularity. On the other hand, it will be shown that, according to such a meaningful set of model parameters, the sufficient condition for exponential growth detailed in Theorem 1 are satisfied, and that the corresponding exponential growth computed according to the approximate model (15) is close to the one coming from simulations of the RRS. The CRS model

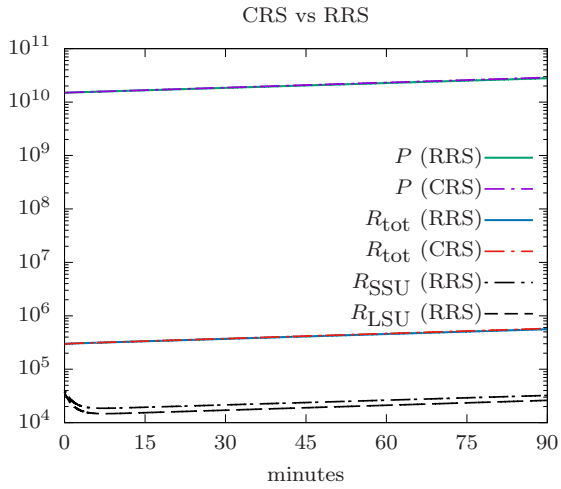

Fig. 2. Accordance between the previous CRS model and the new RRS model together with the new dynamics R_{SSU} and R_{LSU}.

parameters are taken from [20] where they had to comply with the exponential growth rate and cycle parameters experimentally estimated in [21] as well as with novel experimental data presented in [20]. Regards to the RRS parameters, some retain the same meaning of the CRS, and their values have been taken from the existing literature [20], [3]: this is the case for ρ, K_2, γ_p. A second class of parameters are strongly related to the parameters of the CRS: these are the LSU and SSU degradation and production rates γ_{LSU}, γ_{SSU} and k_{LSU}, k_{SSU} set at the same order of magnitude of the total ribosome degradation and production rate in [20], [3]. Finally, the rest of the RRS parameters are not straightforwardly related to any parameters of the CRS, therefore they have been set in order to have protein/ribosome time courses that very well resemble the protein/ribosome time courses of the CRS. In summary, the RRS parameters are: $\rho = 2.02 \cdot 10^{-5}$ rib/aa, $k_{\text{SSU}} = 1.01$ min^{-1}, $\gamma_{\text{SSU}} = 1/3800$ min^{-1}, $k_{\text{LSU}} = 1$ min^{-1}m, $\gamma_{\text{LSU}} = 1/4000$ min^{-1}, $K_2 = 380$ aa/(rib $\cdot$ min), $\gamma_p = 1/3000$ min^{-1}, $k_{\text{on}} = 3 \cdot 10^5$ aa/(rib $\cdot$ min), and $k_{\text{off}} = 0.01$min^{-1}.

The initial conditions have been set as: $P(0) = 1.5 \cdot 10^{10}$aa, $R(0) = 2.6 \cdot 10^5$rib, $R_{\text{SSU}}(0) = 4.07 \cdot 10^4$, $R_{\text{LSU}}(0) = 3.7 \cdot 10^4$rib, $R_{\text{tot}}(0) = 2.97 \cdot 10^5$rib. By taking into account an average cell cycle of 90 minutes, Fig. 2 shows the evolution of the dynamics of the new RRS model, *i.e.* R_{SSU}, R_{LSU}, R, and P. According to the chosen parameter values, SSU and LSU differ of about 10%. Also, it is possible to see the good accordance between the previous CRS model and the new RRS model and the exponential growth (vertical axis in logarithmic scale). With regard to the model parameters, according to the chosen values, all constraints required by Theorem 1 to ensure exponential growth are satisfied (inequalities (17)-(20)): to this end we have exploited the average values $k_{SU} = (k_{SSU}+k_{LSU})/2$ and $\gamma_{SU} = (\gamma_{SSU}+\gamma_{LSU})/2$. Besides, the exponential growth coming from (26) is equal to $6.90 \cdot 10^{-3}$, and it differs from the growth rate computed from the best fitting

exponential of total ribosomes and proteins growth of less than 0.56%.

V. CONCLUSIONS

The tight control of cell growth and cell division is essential for the maintenance of cellular homeostasis and for cell proliferation. Growth is subject to modulation by genetic and environmental conditions, such as nutrient availability. In this work we present an updated model of cellular growth that links the growth rate to protein and RNA synthesis. The updated model explicitly accounts for synthesis of the small and the large ribosomal subunits and their assembly to produce the mature functioning ribosome. The qualitative behavior analysis is carried out providing conditions on model parameters that ensure exponential growth, as well as a way to compute the growth rate.

Ribosome biogenesis is an energetically expensive process. The allocation of proteomic resources to ribosomal production scales linearly with growth rate [22], [23] yielding a specific growth rate-dependent RNA/protein ratio [24]). Inactive ribosomes may act as a "signal" for detecting ribosomes excess and thus adjust their production in order to maximize growth rate [9], [25]. Although the precise molecular nature of the mechanism regulating ribosome biogenesis in yeast are quite different from bacterial cell, the overall control strategy seems to be broadly similar, allowing to finely adjust ribosome assembly rate according to changes in the nutritional status and stress signals (reviewed in [8], [26]). Coupled with the fact that the molecularly detailed feedback regulatory mechanism for ribosome biosynthesis is currently unknown - and could anyway not be implemented in the current low granularity model - we use the ribosome/protein ratio as an effective simplified proxy of the real mechanism allowing straightforward communication among the modules that compose the integrated model. Further developments will allow a molecular blow-up of the biosynthesis of the two ribosomal subunits and their assembly, a key step to produce a system-level, molecular detailed cell growth model.

VI. ACKNOWLEDGMENTS

This work was partially supported by Ministero dell'Istruzione, dell'Università e della Ricerca (MIUR), grant CHRONOS ("Dipartimenti di Eccellenza 2017") and by ISBE.IT, within the Italian Roadmap for ESFRI Research Infrastructures. MdA was supported by Ministero dell'Istruzione, dell'Università e della Ricerca (MIUR), grant CHRONOS ("Dipartimenti di Eccellenza 2017").

REFERENCES

[1] D. White, J. Drummond, and C Fuqua. *The Physiology and Biochemistry of Prokaryotes*. 4th edn. Oxford: Oxford University Press, 2011.

[2] L. Alberghina, L. Mariani, and E. Martegani. Cell cycle modelling. *Biosystems*, 19(1):23–44, 1986.

[3] P. Palumbo, M. Vanoni, F. Papa, S. Busti, M. Wortel, B. Teusink, and L. Alberghina. An integrated model quantitatively describing metabolism, growth and cell cycle in budding yeast. In *Italian Workshop on Artificial Life and Evolutionary Computation*, pages 165–180. Springer, 2017.

[4] Jonathan R Karr, Jayodita C Sanghvi, Derek N Macklin, Miriam V Gutschow, Jared M Jacobs, Benjamin Bolival Jr, Nacyra Assad-Garcia, John I Glass, and Markus W Covert. A whole-cell computational model predicts phenotype from genotype. *Cell*, 150(2):389–401, 2012.

[5] S. Klinge and J.L. Woolford. Ribosome assembly coming into focus. *Nature reviews Molecular cell biology*, 20(2):116–131, 2019.

[6] T.M. Earnest, J. Lai, K. Chen, M.J. Hallock, J.R. Williamson, and Z. Luthey-Schulten. Toward a whole-cell model of ribosome biogenesis: kinetic modeling of ssu assembly. *Biophysical journal*, 109(6):1117–1135, 2015.

[7] P. Palumbo, F. Papa, M. Vanoni, and L. Alberghina. Qualitative behavior of a coarse-grain growth model. In *2019 IEEE 23rd International Conference on Intelligent Engineering Systems (INES)*, pages 41–46. IEEE, 2019.

[8] J. de la Cruz, F. Gómez-Herreros, O. Rodríguez-Galán, V. Begley, M. de la Cruz Muñoz-Centeno, and S. Chávez. Feedback regulation of ribosome assembly. *Curr Genet.*, 64(2):393–404, 2018.

[9] M. Nomura, R. Course, and G. Baugbman. Regulation of the synthesis of ribosomes and ribosomal components. *Annu. Rev. Biochem.*, 53:75–118, 1984.

[10] Y. Arava, Y. Wang, Storey. J.D., C.L. Liu, P.O. Brown, and D. Herschlag. Genome-wide analysis of mrna translation profiles in saccharomyces cerevisiae. *Proc Natl Acad Sci U S A*, 100(7):3889–3894, 2003.

[11] L.M. Hereford and M. Rosbash. Number and distribution of polyadenylated rna sequences in yeast. *Cell*, 10(3):453–462, 1977.

[12] D. Zenklusen, D.R. Larson, and R.H. Singer. Single-rna counting reveals alternative modes of gene expression in yeast. *Nat. Struct. Mol. Biol.*, 15:1263–1271, 2008.

[13] T.A. von der Haar. Quantitative estimation of the global translational activity in logarithmically growing yeast cells. *BMC Syst. Biol.*, 2(87), 2008.

[14] J.R. Warner. The economics of ribosome biosynthesis in yeast. *Trends Biochem. Sci.*, 24(11):437–440, 1999.

[15] F.C. Holstege, E.G. Jennings, J.J. Wyrick, T.I. Lee, C.J. Hengartner, M.R. Green, T.R. Golub, E.S. Lander, and R.A. Young. Dissecting the regulatory circuitry of a eukaryotic genome. *Cell*, 95:717–728, 1998.

[16] D.L.J. Lafontaine. A 'garbage can'for ribosomes: how eukaryotes degrade their ribosomes. *Trends in biochemical sciences*, 35(5):267–277, 2010.

[17] P. Jorgensen, N.P. Edgington, B.L. Schneider, I. Rupes, M. Tyers, and B. Futcher. The size of the nucleus increases as yeast cells grow. *Mol Biol Cell*, 18(9):3523–3532, 2007.

[18] B. Gregory, N. Rahman, A. Bommakanti, M. Shamsuzzaman, M. Thapa, A. Lescure, J.M. Zengel, and L. Lindahl. The small and large ribosomal subunits depend on each other for stability and accumulation. *Life Sci Alliance*, 2(2):e201800150, 2019.

[19] R. Christiano, N. Nagaraj, F. Fröhlich, and T.C. Walther. Global proteome turnover analyses of the yeasts s. cerevisiae and s. pombe. *Cell Rep*, 9(5):1959–1965, 2014.

[20] P. Palumbo, M. Vanoni, V. Cusimano, S. Busti, F. Marano, C. Manes, and L. Alberghina. Whi5 phosphorylation embedded in the g1/s network dynamically controls critical cell size and cell fate. *Nat. Commun.*, 7:ncomms11372, 2016.

[21] S. Di Talia, J.M. Skotheim, J.M. Bean, E.D. Siggia, and F.R. Cross. The effects of molecular noise and size control on variability in the budding yeast cell cycle. *Nature*, 448:947–951, 2007.

[22] E. Metzl-Raz, M. Kafri, G. Yaakov, I. Soifer, Y. Gurvich, and N. Barkai. Principles of cellular resource allocation revealed by condition-dependent proteome profiling. *Elife*, 6:e28034, 2017.

[23] J. Xia, B.J. Sánchez, Y. Chen, K. Campbell, S. Kasvandik, and J. Nielsen. Proteome allocations change linearly with the specific growth rate of saccharomyces cerevisiae under glucose limitation. *Nat. Comm.*, page 2819, 2022.

[24] C. Waldron and F. Lacroute. Effect of growth rate on the amounts of ribosomal and transfer ribonucleic acids in yeast. *J. Bacteriol.*, 122(3):855–865, 1975.

[25] E. Bosdriesz, D. Molenaar, B. Teusink, and F.J. Bruggeman. How fast-growing bacteria robustly tune their ribosome concentration to approximate growth-rate maximization. *FEBS J.*, 282(10):2029–2044, 2015.

[26] D. Shore, S. Zencir, and Albert B. Transcriptional control of ribosome biogenesis in yeast: links to growth and stress signals. *Biochem. Soc. Trans.*, 49(4):1589–1599, 2021.